Cancer-cell-derived exosomes stimulate secretion of growth factors, cytokines and angiopoietic factors by stroma cells, induce proliferation of endothelial cells, and promote angiogenesis in metastatic organs [1,2,5,6]. Thus, cancer-cell-derived exosomes are able to alter the cellular environment to form a metastatic niche and promote metastasis [7,8]. Hence, the tracking fate of cancer-cell-derived exosomes in a metastatic models may help us understand the mechanism of cancer metastasis.

Breast cancer is the most common cancer and the leading cause of cancer death among women worldwide [9]. Metastasis is the major cause of death in breast cancer [9]. Therefore novel biomarkers for detection of early metastasis and therapeutic strategies as well as elucidation of the molecular mechanisms underlying the metastatic process, are urgently required.

In the present report, we describe imaging of transfer of cancer-cell-derived GFP-labeled exosomes *in vitro* and in mouse models of metastatic breast cancer.

## 2. Labeling of exosomes

### 2.1. Markers of exosomes

Several proteins may serve as markers of exosomes [10,11]. Cytoplasmic proteins such as molecular chaperon/heat shock proteins Hsp70 and Hsp90, and ESCRT (endosomal sorting complex required for transport)-associated proteins Alix and Tsg101 exist in exosomes [10,11]. Some membrane-associated proteins such as tetraspanins CD9, CD63 and CD81, which are involved in adhesion and targeting, are found on the surface of exosomes [10,11].

For imaging of exosomes, we used the well-known exosomal marker CD63 to be tagged with green fluorescent protein (GFP). CD63 is mainly expressed in endosomes and exosomes, which are derived from endosomes. Therefore, CD63 can distinguish exosomes from other extracellular vesicles such as apoptotic bodies and microvesicles formed by plasma membrane blebbing. Additionally, since CD63 is anchored to the exosomal membrane, it is suited for tracking exosomes. It is suggested that the expression level of CD63 is related to tumor progression [12]. In fact, it has been observed that plasma exosomes expressing CD63 are significantly elevated in melanoma patients as compared to healthy donors [13]. Imaging tumor-derived exosomes using GFP-tagged CD63 should enable further understanding of the role of exosomes in tumor progression and metastasis.

### 2.2. Fluorescence labeling of exosomes

Small-molecule fluorophores have been used to label exosomes. Including lipophilic carbocyanine dyes such as PKH67 (Ex. 490/Em. 502), PKH26 (Ex. 551/Em. 567), DiI (Ex. 549/Em. 565) and DiR (Ex. 750/Em. 780) [2,5,8]. These dyes present strong and stable fluorescent signals in the exosomal membrane and are useful for monitoring exosome uptake by recipient cells. However, labeling with small-molecule dyes can be used only for purified exosomes from conditioned culture medium and is not useful for tracking cell-to-cell movement of exosomes.

Fluorescent proteins such as GFP or red fluorescent protein (RFP) fused with membrane protein markers can be useful exosome tracers [14]. However, the fluorescence intensity of these proteins depends on the expression level of proteins they are linked to in exosomes. Fluorescent protein-tagged exosomal membrane proteins permit direct visualization of transfer of exosomes from cell to cell in live culture and *in vivo* in tumor models. For imaging of cancer-cell-derived exosomes, we generated mouse breast cancer MMT-060562 (MMT) and human breast cancer MDA-MB-231 cells stably expressing CMV-driven GFP-tagged CD63 using a lentivector system (System Biosciences, Inc., CA; Fig. 1A, B).

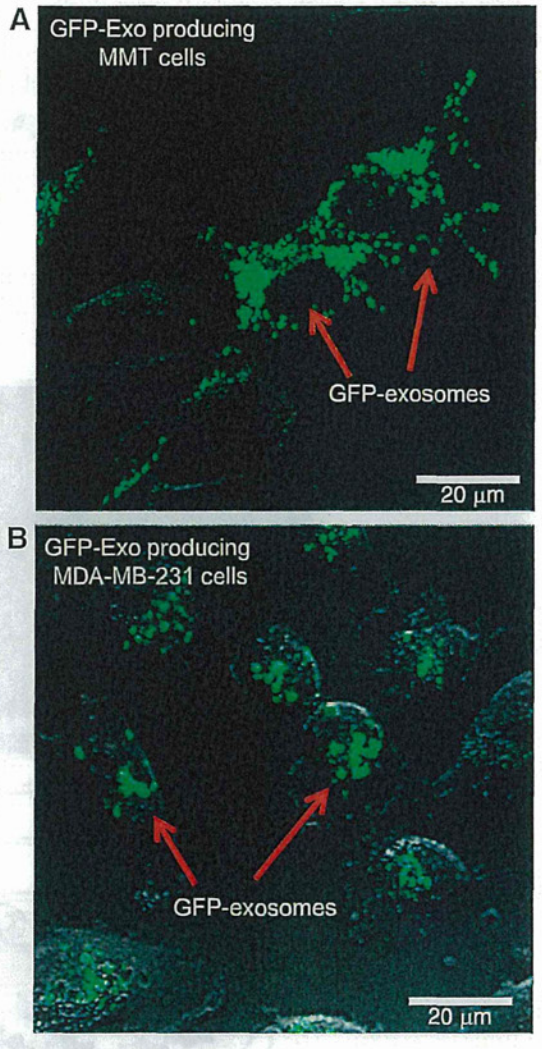


**Fig. 1.** GFP-exosome-producing breast cancer cells. A. GFP-Exo-producing mouse mammary tumor 060562 (MMT) cells. Red arrows indicate GFP-exosomes. B. GFP-Exo-producing MDA-MB-231 cells. Red arrows indicate GFP-exosomes. Scale bar = 20 μm.

## 3. Cell-to-cell transfer of cancer-cell-derived exosomes

Cancer-cell-shed exosomes/microvesicles which transfer genetic and proteomic information to target cells as a way of cell-to-cell communication. For example, primary human glioblastoma cells were observed to secrete microvesicles, including exosomes, into the culture medium by scanning electron microscopy [2]. Glioblastoma microvesicles purified from conditioned medium were internalized by human brain microvascular endothelial (HBMVEC) and delivered functional RNA to the recipient cells [2]. Another study showed that GFP-tagged EGFRvIII, a variant epidermal growth-factor receptor found in some cancer cells, was released from glioma cells *via* microvesicles [6]. Purified GFP-tagged EGFRvIII-containing microvesicles were incorporated into EGFRvIII-negative glioma cells and induced cellular transformation by upregulation of vascular endothelial growth factor (VEGF) and anti-apoptotic proteins and down regulation of a cell-cycle inhibitor [6]. It was suggested that microvesicle transfer of EGFRvIII from a small subpopulation of aggressive cancer cells to

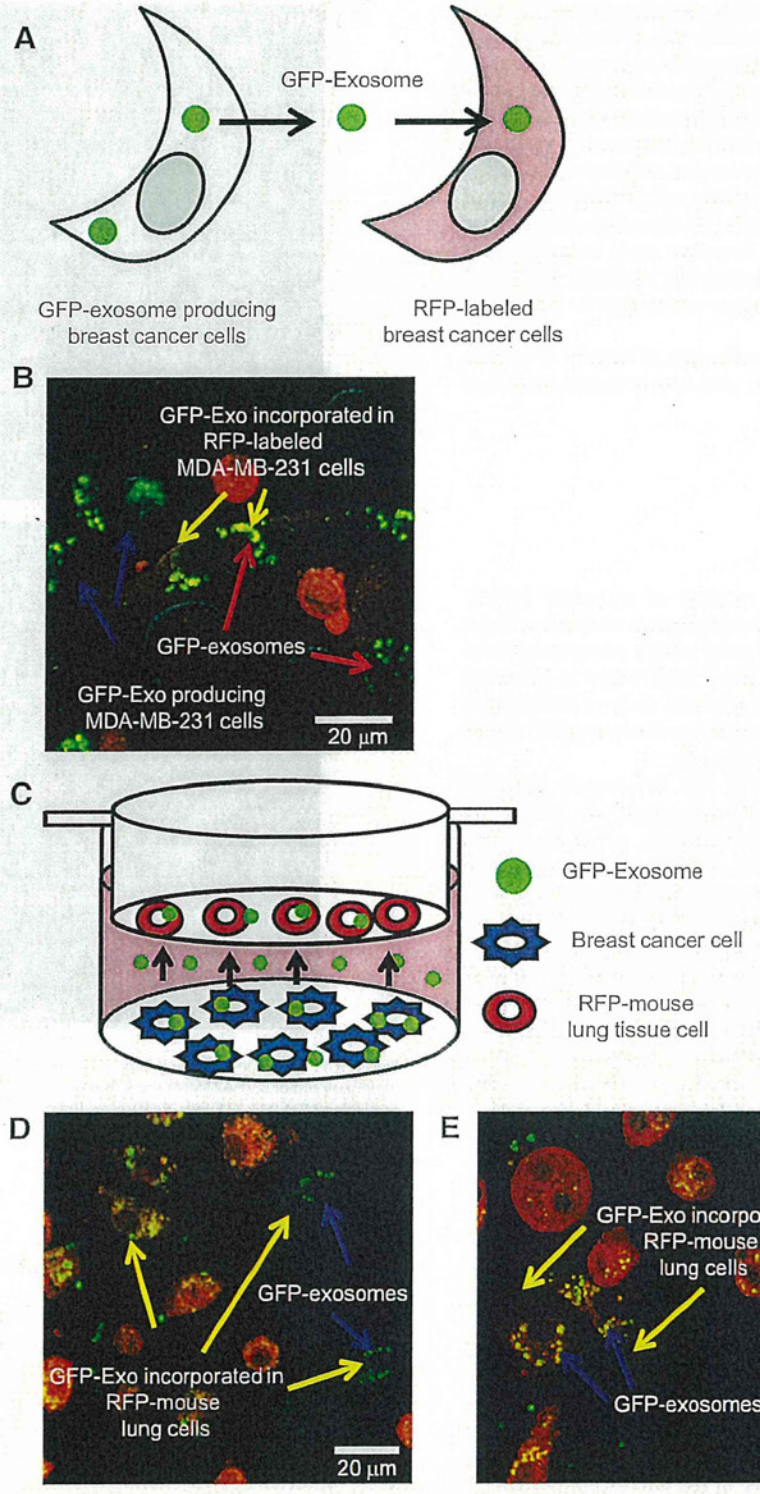


**Fig. 2.** Cell-to-cell transfer of exosomes *in vitro*. A. Diagram of co-culture of GFP-exosome-producing breast cancer cells and RFP-labeled breast cancer cells. B. MDA-MB-231/GFP-Exo cells and RFP-labeled MDA-MB-231 (MDA-MB-231-RFP) cells were mixed (1:1) and cultured for 4 days. Red arrows indicate GFP-exosomes. Yellow arrows indicate GFP-Exo incorporated in RFP-labeled MDA-MB-231 cells. Blue arrows indicate GFP-Exo producing MDA-MB-231 cells. Scale bar = 20 μm. C. Diagram of co-culture of GFP-exosome producing breast cancer cells and RFP-mouse lung tissue cells. D. RFP-lung tissue cells incorporated GFP-exosomes from MMT/GFP-Exo cells during 4 days of co-culture. Blue arrows indicate GFP-exosomes. Yellow arrows indicate GFP-Exo incorporated in RFP-mouse lung cells. Scale bar = 20 μm. E. RFP-lung tissue cells incorporated GFP-exosomes from MDA-MB-231/GFP-Exo cells during 4 days of co-culture. Blue arrows indicate GFP-exosomes. Yellow arrows indicate GFP-Exo incorporated in RFP-mouse lung cells. Scale bar = 20 μm.

a major population of indolent cancer cells promoted glioma progression [6]. It was also reported that colorectal cancer cell-derived microvesicles were enriched in cell cycle-related mRNAs [5]. Purified colorectal cancer cell-derived microvesicles were incorporated in human umbilical vein endothelial cells (HUVECs) and stimulated their proliferation, which can initiate angiogenesis [5].

It is most likely that as carriers of proteins and RNAs from cell to cell, cancer-cell-derived exosomes/microvesicles play an important role in tumor progression. However, there are very few reports on the visualization of cell-to-cell movement of exosomes/microvesicles. Therefore, we attempted to directly visualize the transfer of exosomes from cancer cell to cancer cell or normal cells by imaging GFP-labeled exosomes with confocal laser scanning microscopy (CLSM).

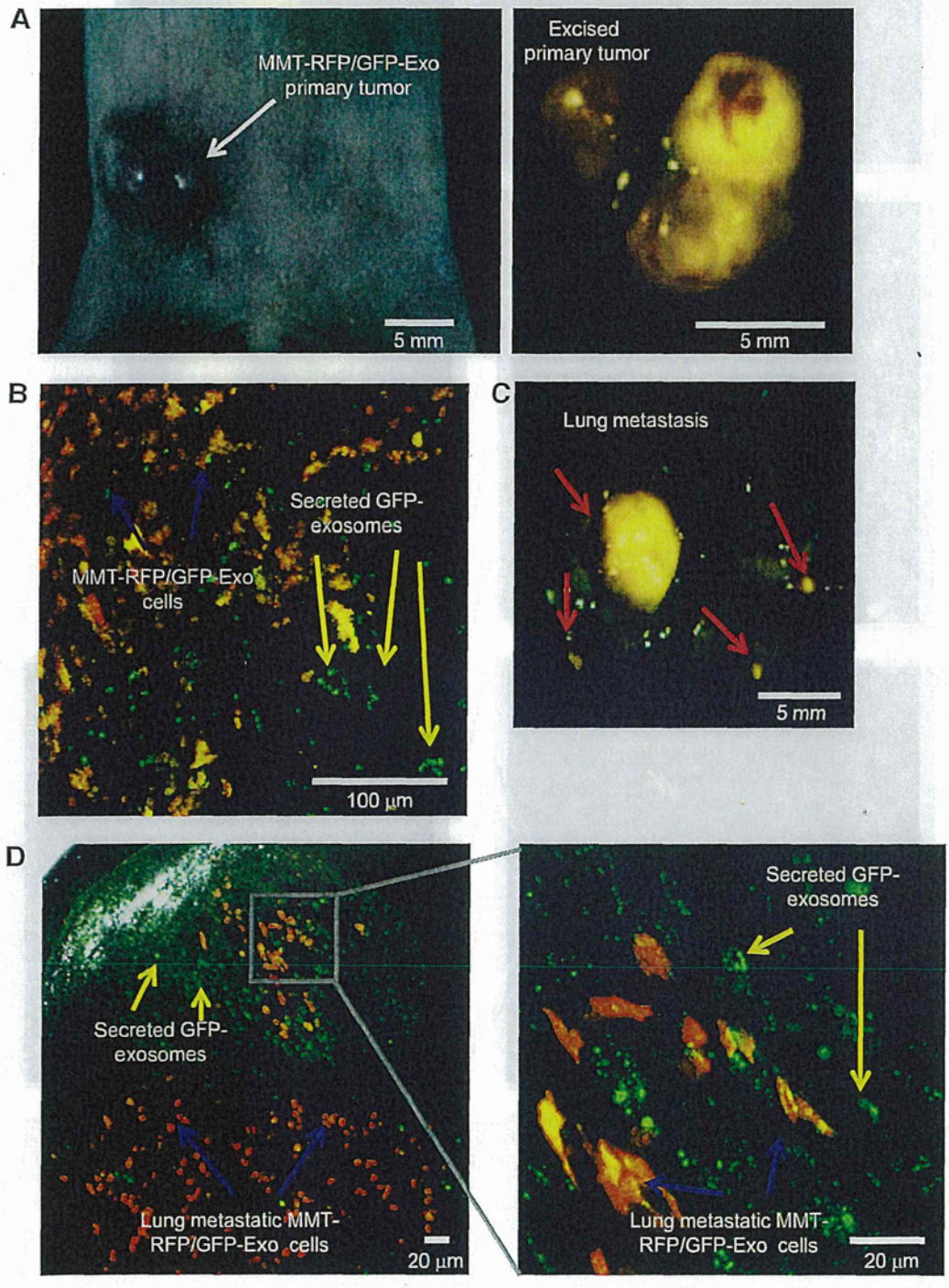


**Fig. 3.** Cancer cells secrete exosomes into the tumor microenvironments in orthotopic MMT breast cancer nude mouse models. A. Bright-field/fluorescence image of MMT-RFP/GFP-Exo primary tumor in mice 10 days after orthotopic injection of cancer cells ($2\times10^6$) in the mammary fat pad (MFP) in mice. Scale bar = 5 mm. B. MMT-RFP/GFP-Exo cells secreted GFP-exosomes in the primary tumor tissue. Blue arrows indicate MMT-RFP/GFP-Exo cells. Yellow arrows indicate secreted GFP-exosomes. Scale bar = 100 μm. C. Bright-field/fluorescence image of MMT-RFP/GFP-Exo tumor metastasized to the lung in mice 5 weeks after orthotopic injection of cells ($2\times10^6$) to the MFP in mice. Red arrows indicate lung metastasis. Scale bar = 5 mm. D. MMT-RFP/GFP-Exo cells secreted GFP-exosomes in the lung metastatic site. Yellow arrows indicate secreted GFP-exosomes. Blue arrows indicate lung metastatic MMT-RFP/GFP-Exo cells. Boxed area in left panel is magnified in right panel. Scale bar = 20 μm.

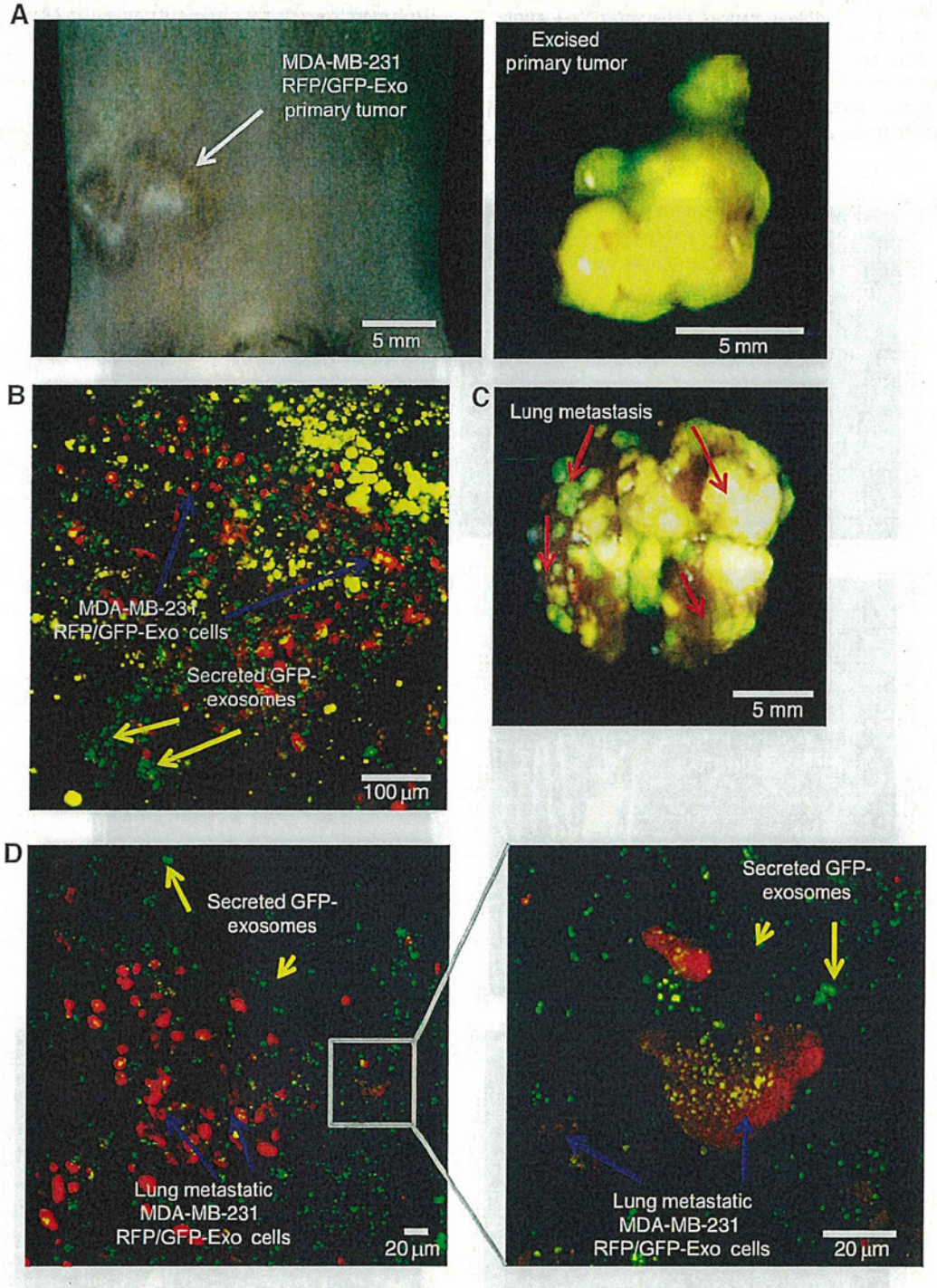


**Fig. 4.** Cancer cells secrete exosomes into the tumor microenvironment in MDA-MB-231 breast cancer models. A. Bright-field/fluorescence image of MDA-MB-231-RFP/GFP-Exo tumor in a mouse 8 weeks after orthotopic injection of cancer cells ($2\times10^6$) to the MFP. Scale bar = 5 mm. B. MDA-MB-231-RFP/GFP-Exo cells secreted GFP-exosomes in the primary tumor tissue. Blue arrows indicate MDA-MB-231-RFP/GFP-Exo cells. Yellow arrows indicate secreted GFP-exosomes. Scale bar = 100 μm. C. Bright-field/fluorescence image of MDA-MB-231-RFP/GFP-Exo lung metastasis 8 weeks after tail vein injection of cells ($2\times10^6$). Red arrows indicate lung metastases. Scale bar = 5 mm. D. MDA-MB-231-RFP/GFP-Exo cells secreted GFP-exosomes at the lung-colonization site. Boxed area in middle panel is magnified in right panel. Yellow arrows indicate secreted GFP-exosomes. Blue arrows indicate lung metastatic MMT-RFP/GFP-Exo cells. Boxed area in left panel is magnified in right panel. Scale bar = 20 μm.

### *3.1. Imaging transfer of exosomes from cancer cell to cancer cell*

In order to observe the transfer of tumor-derived exosomes from cancer cell to cancer cell, we performed co-culture experiments. GFP-exosome-producing breast cancer cells (MMT/GFP-Exo, MDA-MB-231/GFP-Exo) and RFP-labeled breast cancer cells (MMT-RFP, MDA-MB-231-RFP) were mixed (1:1) and cultured for 4 days (Fig. 2A). We observed GFP fluorescence in the cytoplasm of RFP-labeled cells in both mouse

and human breast cancer cell lines demonstrating that RFP breast cancer cells incorporated GFP-exosomes from the breast cancer cells labeled with GFP-CD63 (Fig. 2B). This result shows that cancer-cell-derived exosomes are transferred from cancer cell to cancer cell. Tracking of fluorescent-protein-labeled exosomes may provide clues to understanding the mechanism of tumor progression.

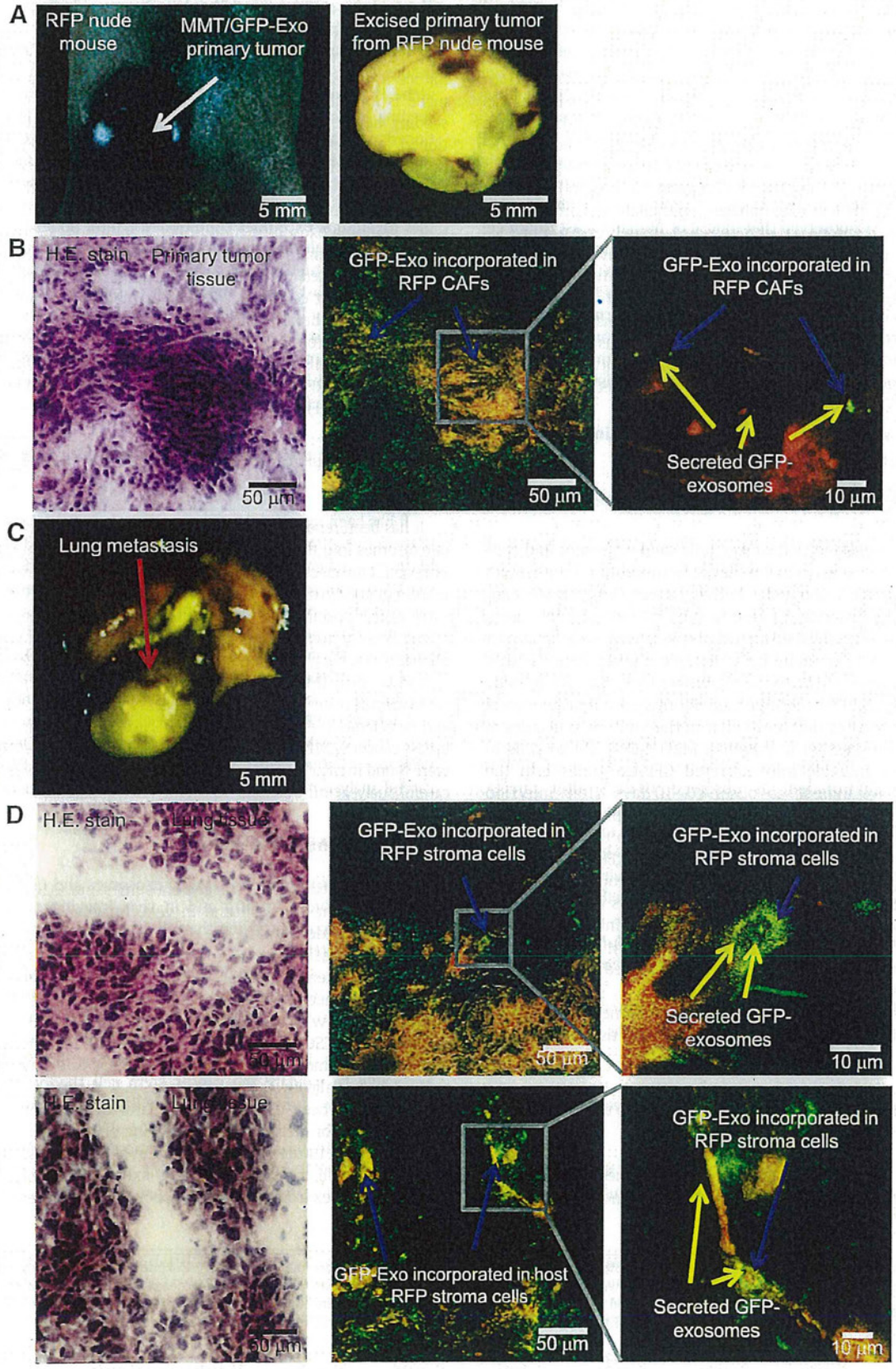

### 3.2. Transfer of cancer-cell-derived exosomes to normal cells

We then examined whether cancer-cell-derived exosomes are incorporated into cells of the lung tissue, which is a common metastatic site of breast cancer, by co-culture of breast cancer cells producing GFP-exosomes (MMT/GFP-Exo, MDA-MB-231/GFP-Exo) and lung tissue cells from RFP transgenic nude mice (AntiCancer Inc., San Diego, CA, Fig. 2C). We used transwell chambers with a 0.4-μm pore PET membrane, which allows transfer of exosomes but blocks most shedded microvesicles (0.1–1 μm in diameter) and apoptotic bodies (>1 μm in diameter) from passing through. We added RFP-lung tissue cells to the chambers and plated GFP-exosome-producing cells on the lower wells and then co-cultured the system for 4 days. RFP-lung tissue cells had macrophage-, epithelial- or fibroblast-like morphologies. We observed that mouse or human breast tumor cell-derived GFP-exosomes were incorporated into endosome-like structures by RFP-lung tissue cells during 4 days of co-culture (Fig. 2D, E). Thus, breast cancer cells secreted exosomes into the extracellular environment which were incorporated by normal tissue cells. Fluorescent-protein-based imaging of exosome transfer may therefore be useful to elucidate intercellular communication between cancer cells and normal cells during tumor metastasis.

## 4. Imaging of cancer-cell-derived exosomes in breast cancer nude-mouse models

### 4.1. Cancer cells secrete exosomes into the tumor microenvironment

It has been suggested that cancer cells shed exosomes and condition their niche *via* exosomal material to promote tumor growth and metastasis. We examined whether cancer cells secrete exosomes into the surrounding tissue in breast cancer models using CLSM imaging. We established an orthotopic mouse model of breast cancer metastasis to the lung by orthotopic implantation of MMT mouse breast cancer cells into the mammary fat pad (MFP) of nude mice (Fig. 3A, C). MMT orthotopic model forms primary tumors and subsequent metastases that are similar to the multiple processes of breast cancer progression in patients. MMT-RFP/GFP-Exo cells in primary tumors in nude mice secreted GFP-exosomes into the extracellular environment as observed 10 days after injection (Fig. 3A, B). Five–six weeks after orthotopic implantation of the MMT-RFP/GFP-Exo cells, the cells metastasized to the lungs of the nude mice (Fig. 3C). The lung-metastatic MMT-RFP/GFP-Exo cells secreted GFP-exosomes into the surrounding environment (Fig. 3D).

GFP-exosome-producing MDA-MB-231-RFP cells (MDA-MB-231-RFP/GFP-Exo) primary tumors secreted exosomes into the extracellular tissue (Fig. 4A, B). Tail vein injection of MDA-MB-231-RFP/GFP-Exo cells resulted lung colonies which also secreted exosomes into the tumor-surrounding tissue (Fig. 4C, D).

Thus, we visualized that the tumor-derived exsomes were secreted from breast cancer cells into the tumor-surrounding tissues, using GFP imaging.

### 4.2. Incorporation of cancer-cell-derived exosomes into tumor-associated cells

Recent studies have proposed that cancer cells shed exosomes and transfer exosomal molecules to other cells during tumor progression. It has been reported that intravenously-injected exosomes, which were produced by mouse breast cancer cells, targeted myeloid precursors in the bone marrow of mice [15]. Breast cancer-derived exosomes induced IL-6 which blocked differentiation of bone marrow dendritic cells [15]. These observations suggest that breast cancer-derived-exosomes mediate tumor-associated immune suppression [15].

Furthermore, it has been indicated that tumor-derived exosomes induce a pre-metastatic niche in murine models. A pre-metastatic niche is a distant target site for metastasis adapted to cancer-cell seeding before the arrival of the first cancer cells [16–18]. Conditioned medium of pancreatic adenocarcinoma cells containing cancer-cell-derived exosomes and soluble factors modulated pre-metastatic organs for cancer cell seeding and growth in rats [7]. Treatment of mice with purified melanoma exosomes demonstrated that melanoma exosomes conditioned lymph nodes to form remote niches for recruitment and growth of melanoma cells [8].

We investigated whether cancer-cell-derived exsomes are incorporated into host cells in breast cancer models. We used RFP nude mice as hosts for breast cancer orthotopic implantation. The RFP nude mouse has red stromal cells surrounding the tumor. The GFP-exsomes targeting host cells included RFP-cancer-associated fibroblasts (RFP-CAFs) and other RFP-stroma cells which may be involved in metastatic niche formation (Fig. 5A–D).

### 4.3. Circulating tumor-derived exosomes in mice with breast cancer metastases

It has been reported that cancer cells released a substantial amount of exosomes into the circulation of cancer patients and animal models of cancer. Cancer-cell-derived exosomes in the circulation are a clinical marker of poor prognosis [4]. Circulating cancer-cell-derived exosomes carry cancer-specific RNAs and proteins and have potential as novel biomarkers for non-invasive detection and diagnosis of cancers such as glioblastoma, lung, prostate and ovarian cancer [2,4,19,20].

We confirmed that breast cancer cells release exosomes into the circulation of mice with lung metastases. We collected blood from mice and detected GFP-exosomes by CLSM. GFP-exosomes,from both mouse breast cancer MMT cells and human breast cancer MDA-MB-231 cells were found in the circulation of host mice (Fig. 6A–C). However, further careful analysis must be done to characterize circulating exosomes.

## 5. Conclusions and perspectives

The combination of GFP-tagged exosomes and CLSM is useful for imaging exosomes *in vitro* and *in vivo*. Imaging of exosomes can contribute to understanding the role of intercellular communication in tumor progression.

The cancer stem cell (CSC) theory proposes that a small subset of cells within a heterogeneous tumor have stem cell-like properties and produce new heterogeneous tumor cells [21–23]. This theory suggests that CSCs lead to metastasis while closely interacting with non-CSCs and niche cells [6,24]. Imaging of exosomes may be applicable to validate the cancer stem cell theory. Tumor-derived exosomes have been viewed as a mediator to condition tissues and prepare niches for metastasis [7,8]. Imaging of exosomes may thus be useful to predict future metastatic location of cancer cells. Subsequent experiments will attempt to detect exosomes in pre-metastatic niches. Imaging exosomes targeting pre-metastatic niches will require

**Fig. 5** Exosomes are transferred from cancer cells to host RFP-mouse cells in tumor tissue. A. Bright-field/fluorescence image of MMT/GFP-Exo primary tumor in a mouse 10 days after orthotopic injection of cancer cells ($2\times10^6$) to the MFP. White arrow indicates MMT/GFP-Exo primary tumor. Scale bar = 5 mm. B. Frozen section of MMT/GFP-Exo primary tumor tissue. Blue arrows indicate GFP-Exo incorporated in RFP cancer-associated fibroblasts (CAFs). Yellow arrows indicate secreted GFP-exosomes. Boxed area in middle panel is magnified in right panel. Scale bar = 10 μm. C. Bright-field/fluorescence image of MMT/GFP-Exo tumor metastasized to the lung in a mouse 6 weeks after orthotopic injection of cancer cells ($2\times10^6$) to the MFP. Red arrow indicates lung metastases. Scale bar = 5 mm. D. Frozen section of MMT-RFP/GFP-Exo tumor metastasized to the lung of a mouse. Blue arrows indicate GFP-Exo incorporated in RFP-stroma cells. Yellow arrows indicate secreted GFP-exosomes. Boxed area in middle panels are magnified in right panel. Scale bar = 10 μm.

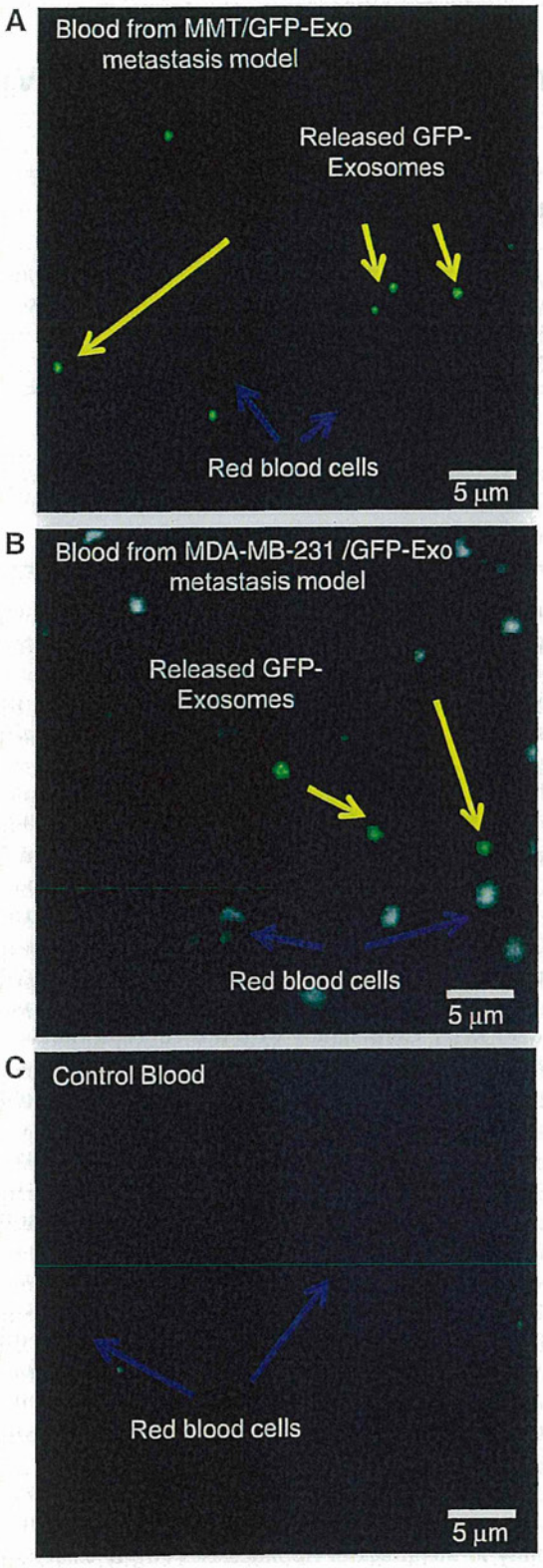


**Fig. 6.** Cancer-cell-derived exosomes circulating in the blood of tumor-bearing mice. A. Blood of mouse that had MMT/GFP-Exo tumor metastasized to lung 6 weeks after orthotopic injection of cells ($2\times10^6$) to the MFP. Yellow arrows indicate released GFP-Exosomes. Blue arrows indicate red blood cells. Scale bar = 5 μm. B. Blood of mouse that had MDA-MB-231-RFP/GFP-Exo tumor colonized in the lung 8 weeks after tail vein injection of cells ($2\times10^6$) to the MFP. Yellow arrows indicate released GFP-Exosomes. Blue arrows indicate red blood cells. Scale bar = 5 μm. C. Blood of untreated mouse. Blue arrows indicate red blood cells. Scale bar = 5 μm.

sufficient circulating exosomes with very bright fluorescence. Refinements of fluorescent proteins and expression systems for exosomal maker proteins should provide improved exosome imaging in the future. We expect that fluorescent protein-based imaging of exosomes will be a powerful tool to elucidate the function of exosomes in tumor metastasis.

## References

[1] J. Ratajczak, M. Wysoczynski, F. Hayek, A. Janowska-Wieczorek, M.Z. Ratajczak, Membrane-derived microvesicles: important and underappreciated mediators of cell-to-cell communication, Leukemia 20 (2006) 1487–1495.
[2] J. Skog, T. Würdinger, S. van Rijn, D.H. Meijer, L. Gainche, M. Sena-Esteves, W.T. Curry Jr., B.S. Carter, A.M. Krichevsky, X.O. Breakefield, Glioblastoma microvesicles transport RNA and proteins that promote tumour growth and provide diagnostic biomarkers, Nat. Cell Biol. 10 (2008) 1470–1476.
[3] H. Valadi, K. Ekström, A. Bossios, M. Sjöstrand, J.J. Lee, J.O. Lötvall, Exosome mediated transfer of mRNAs and microRNAs is a novel mechanism of genetic exchange between cells, Nat. Cell Biol. 9 (2007) 654–659.
[4] G. Rabinowits, C. Gerçel-Taylor, J.M. Day, D.D. Taylor, G.H. Kloecker, Exosomal microRNA: a diagnostic marker for lung cancer, Clin. Lung Cancer 10 (2009) 42–46.
[5] B.S. Hong, J.H. Cho, H. Kim, E.J. Choi, S. Rho, J. Kim, J.H. Kim, D.S. Choi, Y.K. Kim, D. Hwang, Y.S. Gho, Colorectal cancer cell-derived microvesicles are enriched in cell cycle-related mRNAs that promote proliferation of endothelial cells, BMC Genomics 10 (2009) 556.
[6] K. Al-Nedawi, B. Meehan, J. Micallef, V. Lhotak, L. May, A. Guha, J. Rak, Intercellular transfer of the oncogenic receptor EGFRvIII by microvesicles derived from tumour cells, Nat. Cell Biol. 10 (2008) 619–624.
[7] T. Jung, D. Castellana, P. Klingbeil, I. Cuesta Hernández, M. Vitacolonna, D.J. Orlicky, S.R. Roffler, P. Brodt, M. Zöller, CD44v6 dependence of premetastatic niche preparation by exosomes, Neoplasia 11 (2009) 1093–1105.
[8] J.L. Hood, R.S. San, S.A. Wickline, Exosomes released by melanoma cells prepare sentinel lymph nodes for tumor metastasis, Cancer Res. 71 (2011) 3792–3801.
[9] American Cancer Society, Global Cancer Facts & Figures, 2nd Edition American Cancer Society, Atlanta, 2011.
[10] S. Mathivanan, C.J. Fahner, G.E. Reid, R.J. Simpson, ExoCarta 2012: database of exosomal proteins. RNA and lipids, Nucleic Acids Res. 40 (2012) D1241–D1244.
[11] L. Mincheva-Nilsson, V. Baranov, The role of placental exosomes in reproduction, Am. J. Reprod. Immunol. 63 (2010) 520–533.
[12] S. Rorive, X.M. Lopez, C. Maris, A.L. Trepant, S. Sauvage, N. Sadeghi, I. Roland, C. Decaestecker, I. Salmon, TIMP-4 and CD63: new prognostic biomarkers in human astrocytomas, Mod. Pathol. 23 (2010) 1418–1428.
[13] M. Logozzi, A. De Milito, L. Lugini, M. Borghi, L. Calabrò, M. Spada, M. Perdicchio, M.L. Marino, C. Federici, E. Iessi, D. Brambilla, G. Venturi, F. Lozupone, M. Santinami, V. Huber, M. Maio, L. Rivoltini, S. Fais, High levels of exosomes expressing CD63 and caveolin-1 in plasma of melanoma patients, PLoS One 4 (2009) e5219.
[14] M. Mittelbrunn, C. Gutiérrez-Vázquez, C. Villarroya-Beltri, S. González, F. Sánchez-Cabo, M.Á. González, A. Bernad, F. Sánchez-Madrid, Unidirectional transfer of microRNA-loaded exosomes from T cells to antigen-presenting cells, Nat. Commun. 2 (2011) 282.
[15] S. Yu, C. Liu, K. Su, J. Wang, Y. Liu, L. Zhang, C. Li, Y. Cong, R. Kimberly, W.E. Grizzle, C. Falkson, H.G. Zhang, Tumor exosomes inhibit differentiation of bone marrow dendritic cells, J. Immunol. 178 (2007) 6867–6875.
[16] B. Psaila, D. Lyden, The metastatic niche: adapting the foreign soil, Nat. Rev. Cancer 9 (2009) 285–293.
[17] R.N. Kaplan, R.D. Riba, S. Zacharoulis, A.H. Bramley, L. Vincent, C. Costa, D.D. MacDonald, D.K. Jin, K. Shido, S.A. Kerns, Z. Zhu, D. Hicklin, Y. Wu, J.L. Port, N. Altorki, E.R. Port, D. Ruggero, S.V. Shmelkov, K.K. Jensen, S. Rafii, D. Lyden, VEGFR1-positive haematopoietic bone marrow progenitors initiate the pre-metastatic niche, Nature 438 (2005) 820–827.
[18] B. Psaila, R.N. Kaplan, E.R. Port, D. Lyden, Priming the 'soil' for breast cancer metastasis: the pre-metastatic niche, Breast Dis. 26 (2006–2007) 65–74.
[19] P.S. Mitchell, R.K. Parkin, E.M. Kroh, B.R. Fritz, S.K. Wyman, E.L. Pogosova-Agadjanyan, A. Peterson, J. Noteboom, K.C. O'Briant, A. Allen, D.W. Lin, N. Urban, C.W. Drescher, B.S. Knudsen, D.L. Stirewalt, R. Gentleman, R.L. Vessella, P.S. Nelson, D.B. Martin, M. Tewari, Circulating microRNAs as stable blood-based markers for cancer detection, Proc. Natl. Acad. Sci. U. S. A. 105 (2008) 10513–10518.
[20] D.D. Taylor, C. Gercel-Taylor, MicroRNA signatures of tumor-derived exosomes as diagnostic biomarkers of ovarian cancer, Gynecol. Oncol. 110 (2008) 13–21.
[21] H. Clevers, The cancer stem cell: premises, promises and challenges, Nat. Med. 17 (2011) 313–319.
[22] D. Bonnet, J.E. Dick, Human acute myeloid leukemia is organized as a hierarchy that originates from a primitive hematopoietic cell, Nat. Med. 3 (1997) 730–737.
[23] M. Al-Hajj, M.S. Wicha, A. Benito-Hernandez, S.J. Morrison, M.F. Clarke, Prospective identification of tumorigenic breast cancer cells, Proc. Natl. Acad. Sci. U. S. A. 100 (2003) 3983–3988.
[24] C. Grange, M. Tapparo, F. Collino, L. Vitillo, C. Damasco, M.C. Deregibus, C. Tetta, B. Bussolati, G. Camussi, Microvesicles released from human renal cancer stem cells stimulate angiogenesis and formation of lung premetastatic niche, Cancer Res. 71 (2011) 5346–5356.

THE JOURNAL OF BIOLOGICAL CHEMISTRY VOL. 287, NO. 2, pp. 1397–1405, January 6, 2012


# Competitive Interactions of Cancer Cells and Normal Cells via Secretory MicroRNAs*[S]

Received for publication, August 4, 2011, and in revised form, November 23, 2011 Published, JBC Papers in Press, November 28, 2011, DOI 10.1074/jbc.M111.288662

**Nobuyoshi Kosaka**[‡1], **Haruhisa Iguchi**[‡§1], **Yusuke Yoshioka**[‡2], **Keitaro Hagiwara**[‡¶], **Fumitaka Takeshita**[‡], **and Takahiro Ochiya**[‡3]

*From the* [‡]*Division of Molecular and Cellular Medicine, National Cancer Center Research Institute, 5-1-1, Tsukiji, Chuo-ku, Tokyo 104-0045, Japan,* [§]*Pharmacology Research Laboratories, Dainippon Sumitomo Pharma Co., Ltd., 1-98, Kasugadenaka 3-chome, Konohana-ku, Osaka 554-0022, Japan, and the* [¶]*Department of Biological Information, Graduate School of Bioscience and Biotechnology, Tokyo Institute of Technology, Yokohama, Kanagawa 226-8501, Japan*

**Background:** Homeostatic cell competitive system between cancerous cells and non-cancerous cells is considered as the reason for tumor initiation.
**Results:** Exosomal tumor-suppressive microRNAs secreted by non-cancerous cells inhibit the proliferation of cancerous cells.
**Conclusion:** Exosomal tumor-suppressive microRNAs act as an inhibitory signal for cancer cells in a cell-competitive process.
**Significance:** This provides a novel insight into a tumor initiation mechanism.

**Normal epithelial cells regulate the secretion of autocrine and paracrine factors that prevent aberrant growth of neighboring cells, leading to healthy development and normal metabolism. One reason for tumor initiation is considered to be a failure of this homeostatic cell competitive system. Here we identify tumor-suppressive microRNAs (miRNAs) secreted by normal cells as anti-proliferative signal entities. Culture supernatant of normal epithelial prostate PNT-2 cells attenuated proliferation of PC-3M-luc cells, prostate cancer cells. Global analysis of miRNA expression signature revealed that a variety of tumor-suppressive miRNAs are released from PNT-2 cells. Of these miRNAs, secretory miR-143 could induce growth inhibition exclusively in cancer cells *in vitro* and *in vivo*. These results suggest that secretory tumor-suppressive miRNAs can act as a death signal in a cell competitive process. This study provides a novel insight into a tumor initiation mechanism.**

Competitive interactions among cells are the basis of many homeostatic processes in biology. In *Drosophila*, normal epithelial cells compete with transformed ones for individual survival, which is a process called cell competition (1, 2). If a given group of cells was exposed to some stress, it would be separated into subpopulations of cells with different levels of damage. In noncompetitive conditions, cells with severe damage die in a short time, whereas moderately damaged cells survive to the next generation, indicative of the transduction of a negative phenotype. On the other hand, in competitive conditions even slightly damaged cells are eliminated from the cell group because healthy cells, the "winners," convey death signals to damaged cells, the "losers," and the losers reciprocally confer growth signals to the winners. This feed-forward regulation enables the cell population to eradicate abnormal cells and maintain the same number of normal cells in a limited niche.

Oncogenesis is characterized by genetic and metabolic changes reprogramming living cells to undergo uncontrolled proliferation (3). This suggests that the abnormal cells that are originally destined for elimination can survive and expand against the cell competitive regulation, leading to the formation of a tumor mass. Consistently with this concept, Bondar and Medzhitov (4) showed that the cell competition process involves p53, a tumor-suppressive gene, between the hematopoietic stem cells and progenitor cells, suggesting that gene modifications of p53 could disturb the homeostatic mechanism and give rise to tumor initiation. It is conceivable that p53 target genes could be associated with intercellular communication between winners and losers; however, this literature has not answered the question of whether this regulatory system is mediated by contact-dependent or contact-independent manner. More than 10 years ago a pioneer study suggested that non-cancerous cells co-cultured with cancer cells inhibit the growth of cancer cells *in vitro* (5). This result indicated that humoral factors could be involved in cell competition as intercellular communicators (6).

As recently as a few years ago it was believed that RNAs could not behave as extracellular signal molecules because of their vulnerability to the attack of ribonucleases largely existing in body fluid. Evidence is presently increasing to show that miRNAs[4] contained in exosomes are released from mammalian

* This work was supported in part by a grant-in-aid for the Third-Term Comprehensive 10-Year Strategy for Cancer Control, a grant-in-aid for Scientific Research on Priority Areas Cancer from the Ministry of Education, Culture, Sports, Science, and Technology, the Program for Promotion of Fundamental Studies in Health Sciences of the National Institute of Biomedical Innovation, and the Japan Society for the Promotion of Science through the "Funding Program for World-Leading Innovative R&D on Science and Technology (FIRST Program)" initiated by the Council for Science and Technology Policy.
[S] This article contains **supplemental Figs. 1–3.**
[1] Both authors contributed equally to this work.
[2] A Research Fellow of the Japan Society for the Promotion of Science.
[3] To whom correspondence should be addressed: Division of Molecular and Cellular Medicine, National Cancer Center Research Institute, 1-1, Tsukiji, 5-chome, Chuo-ku, Tokyo 104-0045, Japan. Tel.: 81-3-3542-2511 (ext. 4800); Fax: 81-3-3541-2685; E-mail: tochiya@ncc.go.jp.

[4] The abbreviations used are: miRNA, microRNA; CM, conditioned medium; luc, luciferase; MTT, 3-(4,5-dimethylthiazol-2-yl)-2,5-diphenyltetrazolium bromide; QRT-PCR, quantitative real time PCR.

cells and act as a signal transducer (7). It is important that many different tumor-suppressive miRNAs, such as miR-16 and miR-143, are down-regulated in cancer cells, resulting in tumorigenesis, tumor progression, and metastasis (8–11). Taken together, these findings suggest that secretory miRNAs may have favorable aspects for anti-proliferative signals mediating cell competition.

In this report we show that miR-143 expression in normal prostate cells, PNT-2 cells, is higher than that in prostate cancer cells, PC-3M-luc cells, and that miR-143 released from non-cancerous cells transfers growth-inhibitory signals to cancerous cells *in vitro* and *in vivo*. These results suggest that secretory tumor-suppressive miRNAs might be a death signal from winners to losers in the context of cell competition. Secretory miRNAs can be conducive to the maintenance of normal growth and development.

## EXPERIMENTAL PROCEDURES

*Reagents*—Mouse monoclonal anti-KRAS (F234) (sc-30) was purchased from Santa Cruz. Rabbit polyclonal anti-ERK5 (#3372) was purchased from Cell Signaling. Mouse monoclonal anti-actin, clone C4 (MAB1501), was obtained from Millipore. Mouse monoclonal ant-human-CD63 antibody (556019) was purchased from BD Pharmingen. Peroxidase-labeled anti-mouse and anti-rabbit antibodies were included in the Amersham Biosciences ECL PLUS Western blotting Reagents Pack (RPN2124) (GE Healthcare). Synthetic *Caenorhabditis elegans* miRNA cel-miR-39 was synthesized by Qiagen (Valencia, CA). Synthetic hsa-miR-143 (pre-miR-143), the negative control 1 (NC1), has-miR-143 inhibitor molecule (anti-miR-143), and the negative control inhibitor molecule (anti-NC) were purchased from Ambion (Austin, TX). GW4869 was purchased from Calbiochem. Geneticin was purchased from Invitrogen.

*Cell Culture*—PNT-2 cells, immortalized normal adult prostatic epithelial cell line, were purchased from the DS Pharma Biomedical Co., Ltd. (Osaka, Japan). HEK293 cells, a human embryonic kidney cell line (CRL-1573), were obtained from American Type Culture Collection (Manassas, VA). HEK293 cells were cultured in Dulbecco's modified Eagle's medium containing 10% heat-inactivated fetal bovine serum (FBS) and an antibiotic-antimycotic (Invitrogen) at 37 °C in 5% $CO_2$. PNT-2 and the prostate cancer cell line, PC-3M-luc cells, continuously expressing firefly luciferase (Xenogen, Alameda, CA), were cultured in RPMI containing 10% heat-inactivated FBS and an antibiotic-antimycotic at 37 °C in 5% $CO_2$.

*Preparation of Conditioned Medium and Exosomes*—Before the collection of culture medium, cells were washed 3 times with Advanced RPMI containing an antibiotic-antimycotic and 2 mM L-glutamine (medium A), and the medium was switched to fresh medium A. After incubation for 3 days, medium A was collected and centrifuged at 2000 × *g* for 10 min at room temperature. To thoroughly remove cellular debris, the supernatant was centrifuged again at 12,000 × *g* for 30 min at room temperature or filtered through a 0.22-μm filter (Millipore). The conditioned medium (CM) was then used for miRNA extraction and functional assays as well as exosome isolation.

For exosome preparation the CM was ultracentrifuged at 110,000 × *g* for 70 min at 4 °C. The pellets were washed with 11 ml of PBS, and after ultracentrifugation they were resuspended in PBS. The exosome fraction was measured for its protein content using the Micro BCA Protein Assay kit (Thermo Scientific, Wilmington, DE).

*Isolation of MicroRNAs*—Isolation of extracellular and cellular miRNAs was performed using the miRNeasy Mini Kit (Qiagen). Two hundred microliters of conditioned medium or cell lysate was diluted with 1 ml of Qiazol Solution. After 5 min of incubation, 10 μl of 0.1 nM cel-miR-39 was added to each aliquot followed by vortexing for 30 s. Subsequent extraction and filter cartridge work were carried out according to the manufacturer's protocol.

*Quantitative Real Time PCR (QRT-PCR)*—The method for QRT-PCR has been previously described (7). PCR was carried out in 96-well plates using the 7300 Real Time PCR System (Applied Biosystems). All reactions were done in triplicate. All TaqMan MicroRNA Assays were purchased from Applied Biosystems. Cel-miR-39 and RNU6 were used as an invariant control for the CM and cells, respectively.

*Immunoblot Analysis*—SDS-PAGE gels, SuperSep Ace 5–20% (194–15021) (Wako), were calibrated with Precision Plus Protein Standards (161–0375) (Bio-Rad), and anti-KRAS (1:100), anti-ERK5 (1:1000), anti-CD63 (1:200), and anti-actin (1:1000) were used as primary antibodies. The dilution ratio of each antibody is indicated in parentheses. Two secondary antibodies (peroxidase-labeled anti-mouse and anti-rabbit antibodies) were used at a dilution of 1:10,000. Bound antibodies were visualized by chemiluminescence using the ECL PLUS Western blotting detection System (RPN2132) (GE Healthcare), and luminescent images were analyzed by a LuminoImager (LAS-3000; Fuji Film, Inc.). Only gels for CD63 (BD Biosciences) detection were run under non-reducing conditions.

*Plasmids*—The primary-miR-143 expression vector was purchased from TaKaRa BIO. For luciferase-based reporter gene assays, pLucNeo was constructed by inserting a firefly luciferase gene derived from the pGL3-control (Promega) into the pEYFP-1 vector (Clontech) at BglII and AflII sites. The sensor vector for miR-143 was constructed by introducing tandem binding sites with perfect complementarity to miR-143 separated by a four-nucleotide spacer into the NotI site of psiCHECK2 (Promega). The sequences of the binding site are as follows: 5′-AAACCTAGAGCGGCCGCGAGCTACAGTGCT***TCATCTC***AAAGAATTCTTGAGCTACAGTGCT***TCATCTC***AGCGGCCGCTGGCCGCAA-3′ (sense) and 5′-TTGCGGCCAGCGGCCGCTGAGATGAAGCACTGTAGCTCAAGAATTCTTTGAGATGAAGCACTGTAGCTCGCGGCCGCTCTAGGTTT-3′ (antisense). The "seed" sequence of miR-143 is indicated by bold italics. In a mutated miR-143 sensor vector, the seed sequence, TCATCTC, was displaced with GACGAGA. All the plasmids were verified by DNA sequencing.

*Transient Transfection Assays*—Transfections of 10 nM miR-143 mimic and 3 nM anti-miR-143 were accomplished with the DharmaFECT Transfection Reagent (Thermo Scientific) according to the manufacturer's protocol. The total amounts of miRNAs for each transfection were equally adjusted by the addition of NC1 and anti-NC, respectively.

*Establishment of Stable Cell Lines*—Stable HEK293 cell lines that express miR-143 were generated by selection with 300 μg/ml Geneticin. HEK293 cells were transfected with 0.5 μg of the pri-miR-143 expression vector at 90% confluency in 24-well dishes using a Lipofectamine LTX reagent in accordance with the manufacturer's instructions. Twelve hours after the transfection, the cells were re-plated in a 10-cm dish followed by a 3-week selection with the antibiotic. Ten surviving single colonies were picked up from each transfectant and then cultured for another 2 weeks. The cells expressing the largest amount of miR-143 among transfectants were used as miR-143 stably expressing cells.

*Luciferase Reporter Assay*—HEK293 cells were cultured at a density of $1 \times 10^4$ cells/well in 96-well tissue culture plates overnight, and miRNA transfections or the addition of CM was performed. The cells were harvested, and renilla luciferase activity was measured and normalized by firefly luciferase activity (10). All assays were performed in triplicate and repeated at least three times, and the most representative results are shown.

*Cell Growth Assay*—PC-3M-luc cells were seeded at a density of $2 \times 10^3$ cells/well in a 96-well plate. The following day the cells were transfected with mature miRNAs or incubated with a CM. Twenty-four hours later the culture medium of the transfected cells was switched to medium A, whereas the conditioned medium was not changed. After a 3-day culture, cells were harvested for the measurement of firefly luciferase activity. To know the cellular proliferation by the tetrazolium-based colorimetric MTT assay, 20 μl CM of TetraColor ONE (SEIKAGAKU Corp., Tokyo, Japan) was added to each well after 72 h of culture. After 2–4 h of incubation at 37 °C, the optical density was measured at a wavelength of 450 nm using a microplate reader.

*PKH67-labeled Exosome Transfer*—Purified exosomes derived from PNT-2 CM were labeled with a PKH67 green fluorescent labeling kit (Sigma). Exosomes were incubated with 2 μM PKH67 for 5 min, washed 4 times using a 100-kDa filter (Microcon YM-100, Millipore) to remove excess dye, and incubated with PC-3M-luc cells at 37 °C.

*Co-culture Experiment*—In co-culture experiments, $2 \times 10^5$ cells/well of PNT-2 cells were plated in 6-well plates. To stain the PNT-2 cells with BODIPY-TR-ceramide (Invitrogen), 5 μM BODIPY-TR-ceramide in a non-serum culture medium was added and incubated with the cells at 37 °C. After 30 min the cells were rinsed several times with a non-serum culture medium and incubated in a fresh medium at 37 °C for an additional 30 min. After the staining of PNT-2 cells by BODIPY-TR-ceramide, labeling of PC-3M-luc cells with PKH67 was performed in accordance with the manufacturer's instructions. After that, labeled PC-3M-luc cells were added and co-cultured with PNT-2 cells for 12 h at 37 °C.

*Microarray Analysis*—To detect the miRNAs in exosomes and cells derived from PNT-2 and PC-3M-luc cells, 100 ng of total RNA was labeled and hybridized using a human microRNA microarray kit (Agilent Technologies) according to the manufacturer's protocol (Protocol for Use with Agilent MicroRNA Microarrays Version 1.5). Hybridization signals were detected using a DNA microarray scanner (Agilent Technologies), and the scanned images were analyzed using Agilent Feature Extraction software.

*Evaluation of Tumor-suppressive miRNA Delivery to Subcutaneously Implanted Prostate Cancer Cell Line in Mice*—Animal experiments in this study were performed in compliance with the guidelines of the Institute for Laboratory Animal Research, National Cancer Center Research Institute. Seven-week-old male Balb/c athymic nude mice (CLEA Japan, Shizuoka, Japan) were anesthetized by exposure to 3% isoflurane for injections and *in vivo* imaging. Four days ahead of the first CM injection, the anesthetized animals were subcutaneously injected with $5 \times 10^5$ PC-3M-luc cells suspended in 100 μl of sterile Dulbecco's phosphate-buffered saline into each dorsal region. Five hundred μl of CM derived from miR-143-overexpressing HEK293 cells and control cells were daily injected into each tumor from day 0 to 6. For *in vivo* imaging, the mice were administered D-luciferin (150 mg/kg, Promega) by intraperitoneal injection. Ten minutes later, photons from animal whole bodies were counted using the IVIS imaging system (Xenogen) according to the manufacturer's instructions. Data were analyzed using LIVINGIMAGE 2.50 software (Xenogen).

## RESULTS

*Suppression of Prostate Cancer Cell Proliferation by Conditioned Medium Isolated from Non-cancerous Prostatic Cell*—Cell competition is a homeostatic mechanism for the accommodation of an appropriate number of cells in a limited niche or stroma (1). Based on this idea it is possible that the cell competition between normal and abnormal cells frequently occurs in a precancerous state. Of note is that non-cancerous cells suppress cancer cell development by contact-independent interaction (12). For instance, endothelial cells provide the major extracellular heparan sulfate proteoglycan as anti-proliferative signals (12); however, the molecular mechanism by which the other types of cells in a tumor environment associate with cancer cells is not fully understood.

To analyze the mechanism, we treated a hormone-insensitive prostatic carcinoma cell line, PC-3M-luc cells, with a CM from the non-cancerous prostate cell line PNT-2 cells. After a 3-day incubation, the PNT-2 CM inhibited the growth of the PC-3M-luc cells up to ~10% compared with the cell growth treated by fresh culture medium (Fig. 1*A*; compare *lanes 1* and *3*). In contrast, the growth of PC-3M-luc cells incubated in the CM of PC-3M-luc cells themselves showed no inhibitory effect (Fig. 1*A*; compare *lanes 1* and *2*). To determine that the performed treatments did not affect the luciferase activity, we also used the colorimetric MTT assay to measure the cell growth of PC-3M-luc cells. As shown in **supplemental Fig. 1*A***, not only luciferase assay but also MTT assay show the inhibition of PC-3M-luc cell proliferation by the addition of PNT-2 cells derived CM, indicating that our treatment did not affect the luciferase activity. These results indicate that the non-cancerous cells may secrete some molecules that can suppress cancer cell proliferation.

In a recent report we showed that miRNAs contained in exosomes are secreted and that their secretion is tightly regulated by neutral sphingomyelinase 2, which is known to hydrolyze sphingomyelins to generate ceramides and trigger the budding